JACS
JOURNAL OF THE AMERICAN CHEMICAL SOCIETY
pubs.acs.org/JACS
Communication

Programming sp^3 Quantum Defects along Carbon Nanotubes with Halogenated DNA

Xiaojian Wu, Mijin Kim, Lucy J. Wang, Abhindev Kizhakke Veetil, and YuHuang Wang*

Cite This: J. Am. Chem. Soc. 2024, 146, 8826−8831
Read Online
ACCESS | Metrics & More | Article Recommendations | Supporting Information

ABSTRACT: Atomic defect color centers in solid-state systems hold immense potential to advance various quantum technologies. However, the fabrication of high-quality, densely packed defects presents a significant challenge. Herein we introduce a DNA-programmable photochemical approach for creating organic color-center quantum defects on semiconducting single-walled carbon nanotubes (SWCNTs). Key to this precision defect chemistry is the strategic substitution of thymine with halogenated uracil in DNA strands that are orderly wrapped around the nanotube. Photochemical activation of the reactive uracil initiates the formation of sp^3 defects along the nanotube as deep exciton traps, with a pronounced photoluminescence shift from the nanotube band gap emission (by 191 meV for (6,5)-SWCNTs). Furthermore, by altering the DNA spacers, we achieve systematic control over the defect placements along the nanotube. This method, bridging advanced molecular chemistry with quantum materials science, marks a crucial step in crafting quantum defects for critical applications in quantum information science, imaging, and sensing.

Quantum technologies are on the cusp of transformative breakthroughs across diverse fields, including sensing, imaging, and information processing. Central to these innovations is the need for qubit arrays, in which each quantum bit, or qubit, can be individually addressed, consistently produced, and seamlessly integrated into large-scale structures.[1,2] Despite significant progress with ion traps,[3,4] superconducting qubits,[5,6] and entangled photons,[7] it remains a challenge to pack qubits into dense arrays. A promising direction for this challenge is the exploration of organic color centers (OCCs)—sp^3 quantum defects synthesized on the sp^2 carbon lattice of semiconducting single-walled carbon nanotubes (SWCNTs)[8−11]—through advanced defect chemistry and DNA nanotechnologies.[12]

OCCs represent a promising frontier in quantum technologies due to their ability to create deep exciton traps. These molecularly tunable traps emit bright photoluminescence (PL) in the short-wave infrared encompassing telecom wavelengths.[8,13,14] Not only do these exciton traps emit single photons at room temperature,[14] but they can also stabilize trions[15,16] and electron spin[17] and support both optical and electrical pumping,[18,19] offering the potential for engineering photon qubits and efficient quantum interfacing. However, a significant challenge arises in precisely fabricating the OCC arrays on SWCNTs. Although recent advances have enabled lithographic patterning[20] and atomic-level control of individual defects,[21,22] the majority of current methods—largely based on radical reactions[8−11,13,21]—still fall short in placing these defects into dense arrays.

Addressing this challenge requires the precise positioning of reactant molecules on predetermined SWCNT sites prior to reaction initiation—a task that cannot be attained under conventional reaction conditions where reactants are free to move and react randomly in solution. In contrast, synthetic polymers and biopolymers, particularly DNA, have demonstrated their potential in forming ordered structures on SWCNTs, offering a pathway to achieving this positioning control.[23−26] Weisman,[27−29] Zheng,[30] and our team[31] have previously explored using DNA to program defect arrays on SWCNTs. In a notable recent study, Zheng and co-workers utilized singlet oxygen to drive covalent bonding of guanine nucleobases to SWCNTs, achieving the synthesis of sp^2 defect pairs in ordered arrays.[29,30] However, these guanine-based defects only yield shallow exciton traps with spectrally broad emissions that significantly overlap with the nanotube E_{11} emission, limiting their effectiveness for quantum applications.[12,27,30]

In this work, we introduce a DNA-programmable photochemical approach for creating sp^3 quantum defects along the length of SWCNTs. By incorporating halogenated uracil into DNA, we can photochemically trigger the halogenated nucleobase to achieve the synthesis of sp^3 defects with deep exciton traps that function as OCCs. These defects exhibit bright photoluminescence with a significant spectral shift from that of the nanotube host, notably by 191 meV for (6,5)-SWCNTs. This defect emission is substantially more red-shifted from the E_{11} emission than those induced by guanine-induced sp^2 defects,[28,30] closely aligning with the shifts observed in sp^3 defects produced by aryl diazonium[8] and aryl halide chemistries,[13,32] which is desirable for high-purity single-photon generation with the added benefit of being spatially programmable with the DNA.

Received: December 28, 2023
Revised: March 15, 2024
Accepted: March 18, 2024
Published: March 25, 2024

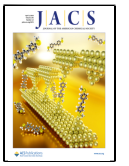

https://doi.org/10.1021/jacs.3c14784
J. Am. Chem. Soc. 2024, 146, 8826−8831

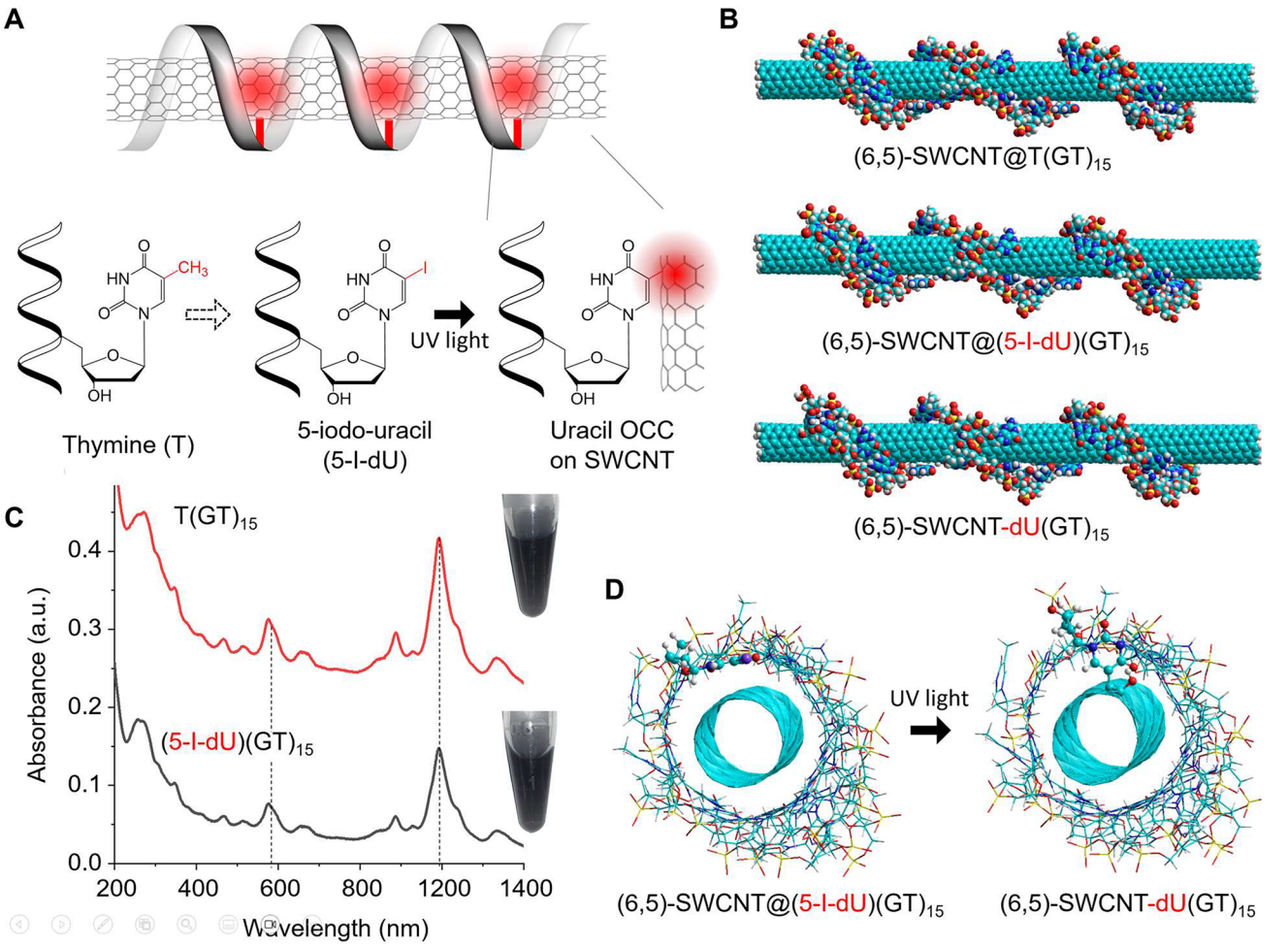

Figure 1. Encoding the reactive sites into a DNA sequence for creating OCCs on SWCNTs. (A) Schematic illustrating the use of engineered DNA sequences to program the OCCs along a nanotube. The reactive sites (highlighted in red) are incorporated by replacing thymine (T) with halogenated uracil (5-I-dU), which is UV-cleavable to form a reactive radical with the nanotube. (B) Molecular models showing the retention of DNA ordered wrapping after covalent attachment. (C) Absorption spectra of the $T(GT)_{15}$ and $(5\text{-I-dU})(GT)_{15}$ ssDNA-dispersed (6,5)-SWCNT samples. For clarity, the spectra are offset. The insets show the corresponding SWCNT solutions prior to a 33-fold dilution for the spectral measurements. (D) Cross-sectional views of (6,5)-SWCNT@$(5\text{-I-dU})(GT)_{15}$ before and after covalent bonding of the dU nucleobase to the nanotube at the iodine leaving site. The bonding atoms and dU are highlighted by ball−sticks.

To program the OCCs along a nanotube, we dispersed individual SWCNTs in water using single-stranded DNA (ssDNA) that had been incorporated with 5-iodouracil (5-I-dU), which is a halogenated and demethylated form of thymine (T). We chose (6,5)-SWCNTs that were wrapped with $(5\text{-I-dU})(GT)_{15}$, hereafter referred to as (6,5)-SWCNT@$(5\text{-I-dU})(GT)_{15}$, as our model system. While the fundamental nucleobases of DNA (G, A, T, and C) generally remain unreactive toward SWCNTs, the C−I bond in 5-I-dU can be cleaved under UV irradiation to produce uracil radical intermediates.[33,34] As we demonstrate in this work, these radicals, once formed, readily react with SWCNTs, leading to the creation of uracil OCCs (Figure 1A). Because uracil and thymine are structurally similar, we used (6,5)-SWCNTs wrapped with $T(GT)_{15}$ (labeled as (6,5)-SWCNT@$T(GT)_{15}$) as a control. Given this structural similarity, the 5-I-dU-modified DNA strand wraps around the nanotube, largely retaining the ordered wrapping structure of the $T(GT)_{15}$ control, even after its halogenated uracil nucleobase covalently bonds to the nanotube to produce the uracil OCC-tailored nanotube, (6,5)-SWCNT-$dU(GT)_{15}$, as depicted by molecular modeling in Figure 1B.

We first experimentally verified that the 5-I-dU-modified DNA can effectively wrap around and disperse SWCNTs just like the unmodified DNA. To fabricate the samples, we sonicated a raw CoMoCAT SWCNT powder in a water solution containing $(5\text{-I-dU})(GT)_{15}$ or $T(GT)_{15}$ and then centrifuged the solutions to remove nanotube bundles and metal catalysts (see details in the Supporting Information). Both the $(5\text{-I-dU})(GT)_{15}$ and $T(GT)_{15}$ dispersed samples attained similar dispersion efficiencies for (6,5)-SWCNTs, as evidenced by their closely matched absorption spectra (Figure 1C). The absorption spectra of both samples present two pronounced peaks at 991 and 565 nm, corresponding to the E_{11} and E_{22} electronic transitions of the (6,5)-SWCNT, respectively, which is the predominant structure in the dispersions. Because the E_{11} peak position is sensitive to the local dielectric environment, which can be affected by a slight change in the DNA morphology on the nanotube surface,[35] the identical E_{11} peak positions indicate that the 5-I-dU incorporation minimally perturbs the DNA wrapping structure on the nanotubes. This observation is further supported by AFM imaging, which confirms the orderly wrapping of the 5-I-dU-modified DNA on the SWCNTs (Figure S1).

https://doi.org/10.1021/jacs.3c14784
J. Am. Chem. Soc. 2024, 146, 8826−8831

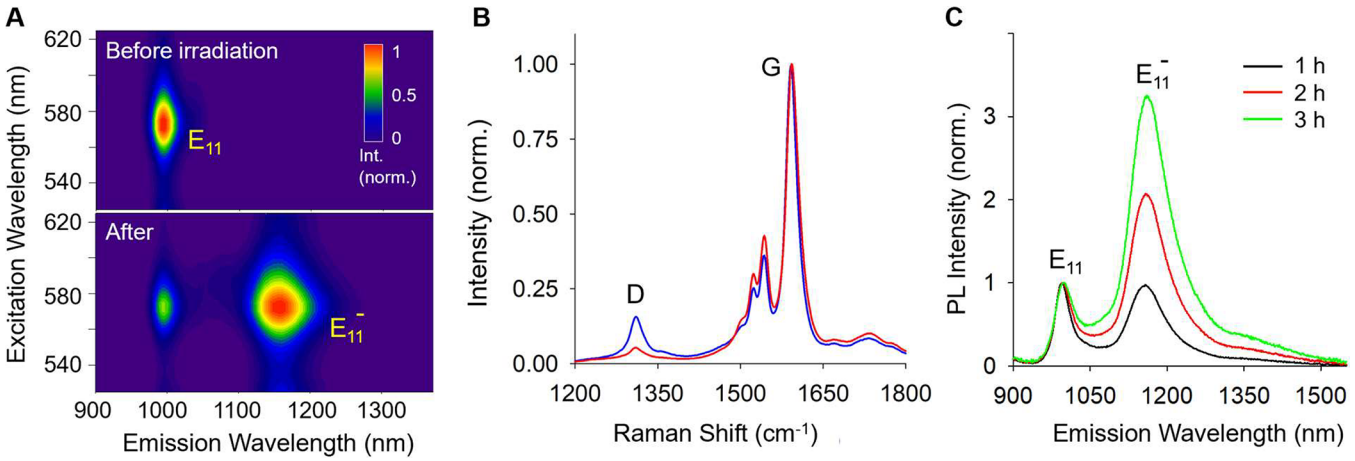

Figure 2. Photochemically triggered creation of OCCs on (5-I-dU)$(GT)_{15}$ ssDNA-wrapped (6,5)-SWCNTs. (A) PL excitation−emission maps of the sample before (top) and after (bottom) exposure to 254 nm UV light. (B) Raman spectra before (red) and after (blue) 3 h of UV irradiation, measured using 532 nm excitation. (C) Photoluminescence spectra within the first 3 h of the UV irradiation, recorded at 565 nm excitation.

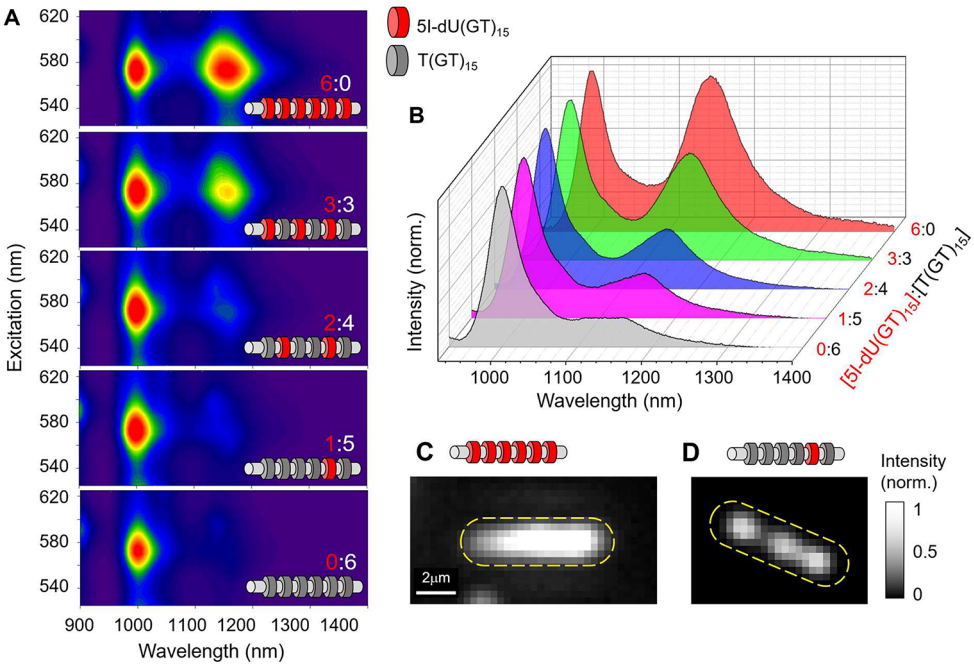

Figure 3. Controlling the defect spacing using inert DNA spacers. (A) PL excitation-emission maps and (B) PL spectra at 565 nm excitation of the DNA/SWCNT samples with different 5-I-dU$(GT)_{15}$:T$(GT)_{15}$ ratios after 1 h reaction. The unmodified DNA sequence, T$(GT)_{15}$, serves as a spacer (depicted in gray in the insets), while the modified sequence, 5-I-dU$(GT)_{15}$, is in red. (C, D) OCC PL images of individual SWCNTs reacted with 5-I-dU$(GT)_{15}$:T$(GT)_{15}$ at ratios of (C) 6:0 and (D) 1:5. Note these images display only OCCs, whereas the nanotube E_{11} PL is filtered using a long-pass filter.

Upon exposure to 254 nm UV light, a photochemical reaction is initiated between 5-I-dU and (6,5)-SWCNT, as illustrated by molecular models shown in Figure 1D. The successful introduction of the OCCs is evident from the rise of the defect PL at 1168 nm, which is red-shifted from the nanotube E_{11} PL by 178 nm (191 meV) (Figure 2A). This observation is consistent with sp^3 quantum defects created by diazonium chemistry.[8,9] Accompanying this new defect emission is an increase in the Raman D/G ratio from 0.053 ± 0.002 to 0.157 ± 0.004 after irradiation, which confirms the covalent nature of these defects (Figure 2B). We find that TEMPO, a known radical quencher, deactivates the creation of the OCC (Figure S2). Additionally, when (6,5)-SWCNT@T$(GT)_{15}$ was exposed to UV light, there was no evidence of new defect PL (Figure S3A). These control experiments consistently suggest that the creation of the sp^3 defects results from a radical-driven reaction between 5-I-dU and the SWCNTs.

The defect PL intensity grows with prolonged exposure to UV light, as shown in Figure 2C. The reaction, signified by rising defect emission over time, is considerably slower for 5-I-dU compared to free aryl halide molecules,[13,32] taking hours rather than minutes. This slowdown can be attributed to DNA-induced spatial constraints. Molecular modeling shows that uracil must rotate from a $\pi-\pi$ stacking to a perpendicular orientation against the nanotube surface for covalent bonding, a process slowed by DNA wrapping (Figure S4). Further, bond length and angle analyses of the OCC support the sp^3

https://doi.org/10.1021/jacs.3c14784
J. Am. Chem. Soc. 2024, 146, 8826−8831

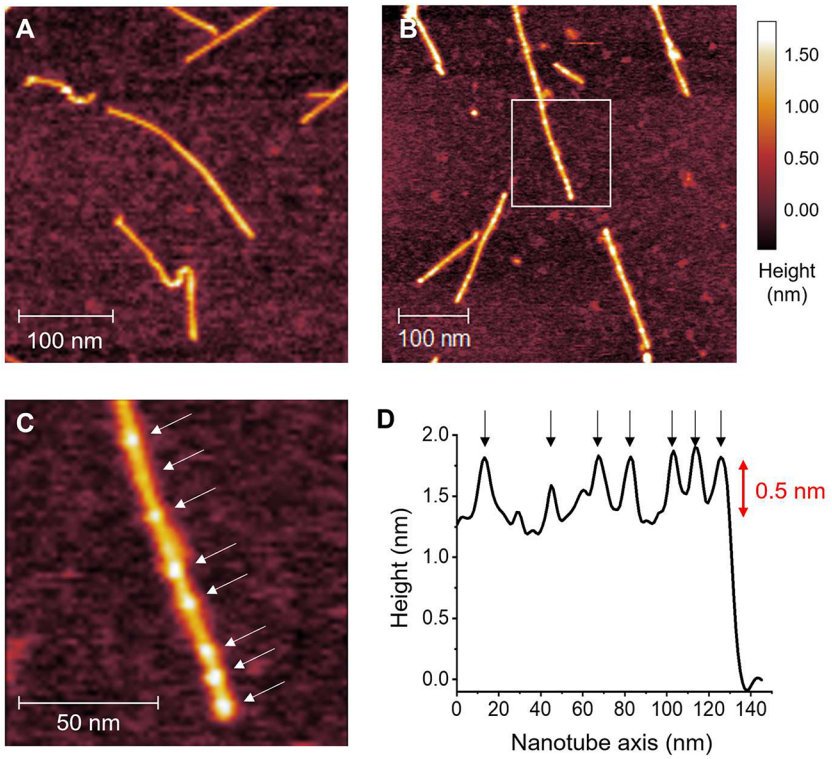

Figure 4. Atomic force microscopy imaging of DNA-programmed quantum defects on individual nanotubes. AFM images of (A) control SWCNT@(5-I-dU)$(GT)_{15}$ and (B, C) (6,5)-SWCNT-dU$(GT)_{15}$ after removal of free DNA. The DNA is visible only in the SWCNT-dU$(GT)_{15}$ sample, where the DNA strands are covalently bonded to the nanotube surface and cannot be removed by DOC. (D) Height profile along the length of the nanotube shown in (C), which is a zoomed-in view corresponding to the marked area in (B).

hybridization nature, aligning with what we observed experimentally (Figure S5).

We then sought to control the spacing between the OCCs on the nanotube using $T(GT)_{15}$ ssDNA as inert spacers. We first dispersed SWCNTs with both (5-I-dU)$(GT)_{15}$ and $T(GT)_{15}$ mixed at concentration ratios varying from 6:0 to 0:6 and subsequently initiated the OCC generation with UV light. We observed a decline in the defect PL intensity as the proportion of DNA spacers increased (Figure 3A). When normalized to the E_{11} value, the defect PL intensity scaled almost linearly with the (5-I-dU)$(GT)_{15}$ to $T(GT)_{15}$ ratio (Figure 3B). Corroborating this observation, single-nanotube PL imaging shows that nanotubes with a high ratio of (5-I-dU)$(GT)_{15}$ to $T(GT)_{15}$ (6:0) displayed uniform OCC emission along their entire length (Figure 3C), although statistical analysis also revealed some heterogeneity (Figures S6 and S7). In contrast, nanotubes with a low 1:5 ratio of (5-I-dU)$(GT)_{15}$ to $T(GT)_{15}$ exhibited sporadic OCC emission sites (Figure 3D), demonstrating effective spacing control.

We further conducted AFM imaging on heavily functionalized SWCNTs in the dry state to reveal the detailed spatial arrangement of DNA-programmed OCCs, which were identifiable at sites of covalent bonding along the nanotube length. After removing free and non-covalently bound DNA (see the Supporting Information), AFM shows that the (6,5)-SWCNT@(5-I-dU)$(GT)_{15}$ control exhibits a uniform height profile consistent with bare nanotubes, signifying the removal of DNA (Figure 4A). In contrast, heavily functionalized SWCNTs display bright spots indicative of covalently attached ssDNA (Figure 4B,C), with heights alternating between 1.8 and 1.2 nm, corresponding to DNA-covered and exposed nanotube sections (Figure 4D). Notably, the observed minimum defect separation (10.2 nm) closely matches the DNA extension (~10.0 nm) derived from molecular modeling (Figure 1B).

The covalently bonded DNA exhibits markedly improved stability, as shown by the surfactant displacement dynamics. Strong surfactants, like sodium deoxycholate (DOC), effectively remove non-covalently bound DNA from nanotubes.[36] As these DNA strands are displaced by surfactant molecules, the changing environment surrounding the nanotube induces spectral shifts in the absorption and PL spectra. For DOC-dispersed (6,5)-SWCNTs, the E_{11} absorption peak is at 981 nm (Figure S8A), while for (6,5)-SWCNT@(5-I-dU)$(GT)_{15}$, it shifts to 991 nm (Figure S8B). Introducing 1 wt % DOC to the latter solution causes the E_{11} band to blue-shift from 991 to 981 nm within 1 min, suggesting rapid DOC replacement of non-covalently bound DNA. However, for the SWCNTs with covalently bonded DNA, adding DOC only partially shifts the E_{11} band to 986 nm (Figure S8C), highlighting the improved stability of DNA-SWCNTs against surfactant displacement.

In conclusion, we have developed a DNA-programmable photochemical method for creating 1D arrays of sp^3 defect color centers in semiconducting SWCNTs by programming reactive uracil sites in DNA sequences that orderly wrap around the nanotube hosts. This uracil chemistry leads to the formation of deep exciton traps desirable for quantum applications, exhibiting substantial photoluminescence spectral shifts from the nanotube PL, notably by 191 meV in (6,5)-SWCNTs, compared to the 27 meV reported with sp^2 defects.[30] The versatility of DNA as a programmable biopolymer, combined with the potential to extend this strategy to other biomolecules, represents a key step in the

https://doi.org/10.1021/jacs.3c14784
J. Am. Chem. Soc. 2024, 146, 8826−8831

chemical engineering of quantum defects. Our work lays the groundwork for crafting quantum defects for a range of applications—from quantum information processing, where the programmable deep exciton traps of OCCs are a promising system for achieving precision color center arrays,[12,14] to chemical sensing and bioimaging,[37,38] bolstered by the biocompatibility and stability conferred by the covalent DNA wrapping.

■ ASSOCIATED CONTENT

Supporting Information

The Supporting Information is available free of charge at https://pubs.acs.org/doi/10.1021/jacs.3c14784.

Detailed experimental procedures, including preparation of DNA-dispersed SWCNT samples, light-activated OCC generation, spectroscopic characterization, removal of free DNA, DNA−DOC exchange, atomic force microscopy, and NIR fluorescence microscopy and imaging; molecular modeling of DNA-coded OCCs in (6,5)-SWCNTs; AFM images of additional control samples; absorption spectra of DNA−surfactant exchange dynamics; additional photoluminescence spectra; hyperspectral imaging and statistical analysis (PDF)

■ AUTHOR INFORMATION

Corresponding Author

YuHuang Wang − *Department of Chemistry and Biochemistry, University of Maryland, College Park, Maryland 20742, United States; Maryland NanoCenter, University of Maryland, College Park, Maryland 20742, United States;* orcid.org/0000-0002-5664-1849; Email: yhw@umd.edu

Authors

Xiaojian Wu − *Department of Chemistry and Biochemistry, University of Maryland, College Park, Maryland 20742, United States*

Mijin Kim − *Department of Chemistry and Biochemistry, University of Maryland, College Park, Maryland 20742, United States; School of Chemistry and Biochemistry, Georgia Institute of Technology, Atlanta, Georgia 30332, United States;* orcid.org/0000-0002-7781-9466

Lucy J. Wang − *Department of Chemistry and Biochemistry, University of Maryland, College Park, Maryland 20742, United States;* Present Address: Princeton University, Princeton, New Jersey 08544, United States

Abhindev Kizhakke Veetil − *Department of Chemistry and Biochemistry, University of Maryland, College Park, Maryland 20742, United States*

Complete contact information is available at: https://pubs.acs.org/10.1021/jacs.3c14784

Notes

The authors declare no competing financial interest.

■ ACKNOWLEDGMENTS

We gratefully acknowledge the National Science Foundation (Grant CHE2204202), the NIH/National Institute of Biomedical Imaging and Bioengineering (Grant R01EB033651), and the NIH/NIBIB (K99/R00 Award R00-EB033580 to M.K.) for partial support of this work.

■ REFERENCES

(1) Hendrickx, N. W.; Lawrie, W. I. L.; Russ, M.; van Riggelen, F.; de Snoo, S. L.; Schouten, R. N.; Sammak, A.; Scappucci, G.; Veldhorst, M. A four-qubit germanium quantum processor. *Nature* **2021**, *591*, 580−585.

(2) Barends, R.; Kelly, J.; Megrant, A.; Veitia, A.; Sank, D.; Jeffrey, E.; White, T. C.; Mutus, J.; Fowler, A. G.; Campbell, B.; Chen, Y.; Chen, Z.; Chiaro, B.; Dunsworth, A.; Neill, C.; O'Malley, P.; Roushan, P.; Vainsencher, A.; Wenner, J.; Korotkov, A. N.; Cleland, A. N.; Martinis, J. M. Superconducting quantum circuits at the surface code threshold for fault tolerance. *Nature* **2014**, *508*, 500−3.

(3) Kielpinski, D.; Monroe, C.; Wineland, D. J. Architecture for a large-scale ion-trap quantum computer. *Nature* **2002**, *417*, 709−11.

(4) Monroe, C.; Kim, J. Scaling the ion trap quantum processor. *Science* **2013**, *339*, 1164−9.

(5) Clarke, J.; Wilhelm, F. K. Superconducting quantum bits. *Nature* **2008**, *453*, 1031−42.

(6) Devoret, M. H.; Schoelkopf, R. J. Superconducting circuits for quantum information: an outlook. *Science* **2013**, *339*, 1169−74.

(7) Yan, Z.; Zhang, Y.-R.; Gong, M.; Wu, Y.; Zheng, Y.; Li, S.; Wang, C.; Liang, F.; Lin, J.; Xu, Y.; Guo, C.; Sun, L.; Peng, C.-Z.; Xia, K.; Deng, H.; Rong, H.; You, J. Q.; Nori, F.; Fan, H.; Zhu, X.; Pan, J.-W. Strongly correlated quantum walks with a 12-qubit superconducting processor. *Science* **2019**, *364*, 753−756.

(8) Piao, Y.; Meany, B.; Powell, L. R.; Valley, N.; Kwon, H.; Schatz, G. C.; Wang, Y. Brightening of carbon nanotube photoluminescence through the incorporation of sp^3 defects. *Nat. Chem.* **2013**, *5*, 840−5.

(9) Brozena, A. H.; Kim, M.; Powell, L. R.; Wang, Y. Controlling the optical properties of carbon nanotubes with organic colour-centre quantum defects. *Nat. Rev. Chem.* **2019**, *3*, 375−392.

(10) Gifford, B. J.; Kilina, S.; Htoon, H.; Doorn, S. K.; Tretiak, S. Controlling Defect-State Photophysics in Covalently Functionalized Single-Walled Carbon Nanotubes. *Acc. Chem. Res.* **2020**, *53*, 1791−1801.

(11) Shiraki, T.; Miyauchi, Y.; Matsuda, K.; Nakashima, N. Carbon Nanotube Photoluminescence Modulation by Local Chemical and Supramolecular Chemical Functionalization. *Acc. Chem. Res.* **2020**, *53*, 1846−1859.

(12) Wang, Y. Engineering defects with DNA. *Science* **2022**, *377*, 473−474.

(13) Kwon, H.; Furmanchuk, A.; Kim, M.; Meany, B.; Guo, Y.; Schatz, G. C.; Wang, Y. Molecularly Tunable Fluorescent Quantum Defects. *J. Am. Chem. Soc.* **2016**, *138*, 6878−85.

(14) He, X.; Hartmann, N. F.; Ma, X.; Kim, Y.; Ihly, R.; Blackburn, J. L.; Gao, W.; Kono, J.; Yomogida, Y.; Hirano, A.; Tanaka, T.; Kataura, H.; Htoon, H.; Doorn, S. K. Tunable room-temperature single-photon emission at telecom wavelengths from sp3 defects in carbon nanotubes. *Nat. Photonics* **2017**, *11*, 577−582.

(15) Brozena, A. H.; Leeds, J. D.; Zhang, Y.; Fourkas, J. T.; Wang, Y. Controlled defects in semiconducting carbon nanotubes promote efficient generation and luminescence of trions. *ACS Nano* **2014**, *8*, 4239−47.

(16) Kwon, H.; Kim, M.; Nutz, M.; Hartmann, N. F.; Perrin, V.; Meany, B.; Hofmann, M. S.; Clark, C. W.; Htoon, H.; Doorn, S. K.; Hogele, A.; Wang, Y. Probing Trions at Chemically Tailored Trapping Defects. *ACS. Cent. Sci.* **2019**, *5*, 1786−1794.

(17) Chen, J.-S.; Trerayapiwat, K. J.; Sun, L.; Krzyaniak, M. D.; Wasielewski, M. R.; Rajh, T.; Sharifzadeh, S.; Ma, X. Long-lived electronic spin qubits in single-walled carbon nanotubes. *Nat. Commun.* **2023**, *14*, 848.

(18) Xu, B.; Wu, X.; Kim, M.; Wang, P.; Wang, Y. Electroluminescence from 4-nitroaryl organic color centers in semiconducting single-wall carbon nanotubes. *J. Appl. Phys.* **2021**, *129*, 044305.

(19) Li, M.-K.; Riaz, A.; Wederhake, M.; Fink, K.; Saha, A.; Dehm, S.; He, X.; Schöppler, F.; Kappes, M. M.; Htoon, H.; Popov, V. N.; Doorn, S. K.; Hertel, T.; Hennrich, F.; Krupke, R. Electroluminescence from Single-Walled Carbon Nanotubes with Quantum Defects. *ACS Nano* **2022**, *16*, 11742−11754.

(20) Huang, Z.; Powell, L. R.; Wu, X.; Kim, M.; Qu, H.; Wang, P.; Fortner, J. L.; Xu, B.; Ng, A. L.; Wang, Y. Photolithographic Patterning of Organic Color-Centers. *Adv. Mater.* **2020**, *32*, 1906517.
(21) Settele, S.; Berger, F. J.; Lindenthal, S.; Zhao, S.; El Yumin, A. A.; Zorn, N. F.; Asyuda, A.; Zharnikov, M.; Högele, A.; Zaumseil, J. Synthetic control over the binding configuration of luminescent sp3-defects in single-walled carbon nanotubes. *Nat. Commun.* **2021**, *12*, 2119.
(22) Wang, P.; Fortner, J.; Luo, H.; Kłos, J.; Wu, X.; Qu, H.; Chen, F.; Li, Y.; Wang, Y. Quantum Defects: What Pairs with the Aryl Group When Bonding to the sp2 Carbon Lattice of Single-Wall Carbon Nanotubes? *J. Am. Chem. Soc.* **2022**, *144*, 13234−13241.
(23) O'Connell, M. J.; Boul, P.; Ericson, L. M.; Huffman, C.; Wang, Y.; Haroz, E.; Kuper, C.; Tour, J.; Ausman, K. D.; Smalley, R. E. Reversible water-solubilization of single-walled carbon nanotubes by polymer wrapping. *Chem. Phys. Lett.* **2001**, *342*, 265−271.
(24) Zheng, M.; Jagota, A.; Strano, M. S.; Santos, A. P.; Barone, P.; Chou, S. G.; Diner, B. A.; Dresselhaus, M. S.; McLean, R. S.; Onoa, G. B.; Samsonidze, G. G.; Semke, E. D.; Usrey, M.; Walls, D. J. Structure-based carbon nanotube sorting by sequence-dependent DNA assembly. *Science* **2003**, *302*, 1545−8.
(25) Zhang, J.; Landry, M. P.; Barone, P. W.; Kim, J.-H.; Lin, S.; Ulissi, Z. W.; Lin, D.; Mu, B.; Boghossian, A. A.; Hilmer, A. J.; Rwei, A.; Hinckley, A. C.; Kruss, S.; Shandell, M. A.; Nair, N.; Blake, S.; Şen, F.; Şen, S.; Croy, R. G.; Li, D.; Yum, K.; Ahn, J.-H.; Jin, H.; Heller, D. A.; Essigmann, J. M.; Blankschtein, D.; Strano, M. S. Molecular recognition using corona phase complexes made of synthetic polymers adsorbed on carbon nanotubes. *Nat. Nanotechnol.* **2013**, *8*, 959−968.
(26) Roxbury, D.; Jagota, A.; Mittal, J. Structural Characteristics of Oligomeric DNA Strands Adsorbed onto Single-Walled Carbon Nanotubes. *J. Phys. Chem. B* **2013**, *117*, 132−140.
(27) Zheng, Y.; Alizadehmojarad, A. A.; Bachilo, S. M.; Weisman, R. B. Guanine-Specific Chemical Reaction Reveals ssDNA Interactions on Carbon Nanotube Surfaces. *J. Phys. Chem. Lett.* **2022**, *13*, 2231−2236.
(28) Zheng, Y.; Kim, Y.; Jones, A. C.; Olinger, G.; Bittner, E. R.; Bachilo, S. M.; Doorn, S. K.; Weisman, R. B.; Piryatinski, A.; Htoon, H. Quantum Light Emission from Coupled Defect States in DNA-Functionalized Carbon Nanotubes. *ACS Nano* **2021**, *15*, 10406−10414.
(29) Zheng, Y.; Bachilo, S. M.; Weisman, R. B. Controlled Patterning of Carbon Nanotube Energy Levels by Covalent DNA Functionalization. *ACS Nano* **2019**, *13*, 8222−8228.
(30) Lin, Z.; Beltran, L. C.; De los Santos, Z. A.; Li, Y.; Adel, T.; Fagan, J. A.; Hight Walker, A. R.; Egelman, E. H.; Zheng, M. DNA-guided lattice remodeling of carbon nanotubes. *Science* **2022**, *377*, 535−539.
(31) Wang, Y.; Wu, X.; Kwon, H.; Kim, M. Chemically coded quantum emitters and photochemical methods of creating same. US 20180265779 A1, 2019.
(32) Wu, X.; Kim, M.; Kwon, H.; Wang, Y. Photochemical Creation of Fluorescent Quantum Defects in Semiconducting Carbon Nanotube Hosts. *Angew. Chem.* **2018**, *130*, 656−661.
(33) Norris, C. L.; Meisenheimer, P. L.; Koch, T. H. Mechanistic studies of the 5-iodouracil chromophore relevant to its use in nucleoprotein photo-cross-linking. *J. Am. Chem. Soc.* **1996**, *118*, 5796−5803.
(34) Willis, M.; Hicke, B.; Uhlenbeck, O.; Cech, T.; Koch, T. Photocrosslinking of 5-iodouracil-substituted RNA and DNA to proteins. *Science* **1993**, *262*, 1255−1257.
(35) Heller, D. A.; Jeng, E. S.; Yeung, T. K.; Martinez, B. M.; Moll, A. E.; Gastala, J. B.; Strano, M. S. Optical detection of DNA conformational polymorphism on single-walled carbon nanotubes. *Science* **2006**, *311*, 508−11.
(36) Zheng, Y.; Bachilo, S. M.; Weisman, R. B. Enantiomers of Single-Wall Carbon Nanotubes Show Distinct Coating Displacement Kinetics. *J. Phys. Chem. Lett.* **2018**, *9*, 3793−3797.
(37) Metternich, J. T.; Wartmann, J. A. C.; Sistemich, L.; Nißler, R.; Herbertz, S.; Kruss, S. Near-Infrared Fluorescent Biosensors Based on Covalent DNA Anchors. *J. Am. Chem. Soc.* **2023**, *145*, 14776−14783.
(38) Kim, M.; Chen, C.; Yaari, Z.; Frederiksen, R.; Randall, E.; Wollowitz, J.; Cupo, C.; Wu, X.; Shah, J.; Worroll, D.; Lagenbacher, R. E.; Goerzen, D.; Li, Y.-M.; An, H.; Wang, Y.; Heller, D. A. Nanosensor-based monitoring of autophagy-associated lysosomal acidification in vivo. *Nat. Chem. Biol.* **2023**, *19*, 1448−1457.

https://doi.org/10.1021/jacs.3c14784
J. Am. Chem. Soc. 2024, 146, 8826−8831